**Regional Studies in Marine Science**
September 2022, Volume 55 Pages 102537 (17p.)
https://doi.org/10.1016/j.rsma.2022.102537
https://archimer.ifremer.fr/doc/00786/89752/

Archimer
https://archimer.ifremer.fr

# Characterisation of long-term evolution (1950–2016) and vulnerability of Mayotte's shoreline using aerial photographs and a multidisciplinary vulnerability index

Courteille Marine [1, 2, *], Jeanson Matthieu [1, 3], Collin Antoine [2], James Dorothée [2], Claverie Thomas [1, 4], Charpentier Michel [5], Gairin Emma [6], Trouillefou Malika [7], Giraud-Renard Eléa [7], Dolique Franck [7], Lecchini David [6]

[1] University Center of Mayotte CUFR, Mayotte, France
[2] EPHE-PSL University, Coastal GeoEcological Lab, 35800 Dinard, France
[3] ESPACE-DEV, Univ Montpellier, IRD, Univ Antilles, Univ Guyane, Univ Réunion, Montpellier, France
[4] MARBEC, University of Montpellier, CNRS, IFREMER, IRD, Montpellier, France
[5] Association Les Naturalistes, environnement et partimoine de Mayotte, Mayotte, France
[6] CRIOBE, EPHE, Université PSL, UPVD, CNRS, UAR CRIOBE, BP1013, 98729 Moorea, French Polynesia
[7] Laboratoire de Biologie des Organismes et Ecosystèmes Aquatiques (BOREA), Université des Antilles - MNHN - CNRS 8067 - SU - IRD 207 – UCN, Guadeloupe & Martinique, France

* Corresponding author : Marine Courteille, email address : marine.courteille1@hotmail.com

**Abstract :**

The shoreline is often at the interface of a combination of physical, ecological, and socio-economic forcing agents. Monitoring the shoreline changes across time is crucial to understand the causes of its evolution and put in place management measures. The analysis of aerial photographs from 1950 to 2016 at Mayotte Island (Indian Ocean) showed that the shoreline urbanisation is still low (6%) compared to the worldwide trend. However, a faster increase happened recently (from 3% in 1989 to 6% in 2016) owing to a strong demographic growth and socio-economic development. A multidisciplinary index was developed to assess the vulnerability of four study sites – Bandrélé, M'tsamboro, N'gouja, and Sakouli – (representative sites of beaches with fringing reefs throughout Mayotte with varying levels of urbanisation). The vulnerability of Bandrélé was lower than that of the other sites due to the presence of a mangrove at the back of the beach which plays a key role of buffer between the land and sea. M'tsamboro was the site with the highest anthropogenic pressure and highest vulnerability. Overall, as most of the shoreline is still natural at Mayotte, a sound management advice would be to put in place conservation measures to preserve natural coastal habitats, such as beaches, mangroves, seagrass beds, and coral reefs. The multidisciplinary vulnerability index developed in this study can be a useful tool to help coastal managers in the decision-making and prioritisation of actions to undertake on the shore.

Please note that this is an author-produced PDF of an article accepted for publication following peer review. The definitive publisher-authenticated version is available on the publisher Web site.

## Graphical abstract

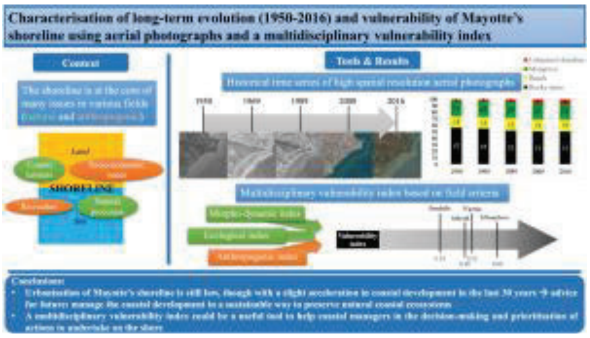


## Highlights

► Urbanisation of Mayotte's shoreline increased mainly from 1989 to 2016. ► Urbanisation of Mayotte's shoreline is still low compared with the worldwide trend. ► Mangroves, coral reefs and seagrass beds reduce the vulnerability of nearby beaches. ► Urbanisation and anthropogenic pressures increase the vulnerability of beaches. ► Conservation of natural protective coastal ecosystems is crucial in Mayotte.

**Keywords** : Shoreline, Urbanisation, Erosion, Coastal management, Airborne imagery, Vulnerability, Mayotte

Please note that this is an author-produced PDF of an article accepted for publication following peer review. The definitive publisher-authenticated version is available on the publisher Web site.

# 1. Introduction

The shoreline is at the core of many issues and activities in different fields: natural processes taking place along the shoreline, habitats for several organisms, socio-economic issues and recreation for humans through ecosystem services (Turner and Schaafsma, 2015). The shoreline is often defined as the physical interface of land and water (Dolan et al., 1980). However, this definition may not be sufficient for users and managers, notably in light of the dynamic nature of the shoreline (Boak and Turner, 2005): more facets of the shoreline must be considered. Several natural factors influence the shoreline's position on short- and long-terms, such as the changing water level (e.g., waves, tides, etc.), the cross- and long-shore movement of sediments (Boak and Turner, 2005), as well as anthropogenic factors, such as embankments and other infrastructures modifying the shoreline. Shoreline evolution is an important topic in this rapidly changing world. Indeed, in addition to being a physical boundary, the shoreline is also an ecotone between terrestrial and marine systems, with numerous coastal ecosystems such as mangroves, seagrass beds, reef flat, etc. (Ray and Hayden, 1992). Moreover, about 40% of the world's population live within 100 km of the coast, and 10% in coastal areas that are less than 10 meters above sea level (United Nations, 2017), making the shoreline a key location for human activities. However, the shoreline is exposed to numerous physical factors that can destabilise it. Background swell and waves, storm-induced sea surges, and other weather-related forces can cause coastal erosion. In addition to background weather variability, global climate change is driving an intensification in the frequency and strength of extreme weather events as well as causing a rise in the sea level, predicted to reach 0.84 m (RCP8.5 scenario) by 2100 relative to 1986-2005 (IPCC, 2019). These are already having and will continue to have strong impacts on shoreline stability. Superposed to these natural changes, local and direct human actions can reinforce erosional processes and shoreline instability (Cooper and Jackson, 2019). These local actions and their impact must be better characterised: analyses of the variability in natural and local human factors and their links to shoreline erosion/accretion trends and vulnerability are important for numerous coastal applications in several fields, such as coastal environment conservation and coastal management (Boak and Turner, 2005), all the more in islands which, by definition, are limited by shores. Coastal erosion is a worldwide issue, and French overseas territories are particularly vulnerable because of their tropical settings with extreme weather and their specific socio-economic and cultural background. Several tools were already used (alone or combined) to assess shoreline evolution worldwide, including field observation with physical clues of past phenomena (e.g., Letortu et al., 2014; Madi Moussa et al., 2019), airborne imagery (e.g., Rault et al., 2020; Gairin et al., 2021), and spaceborne imagery (e.g., Besset et al., 2019; Gairin et al., 2021).

Assessing the vulnerability of the shore is also fundamental for coastal management. Vulnerability is defined by the IPCC (2019) as "The propensity or predisposition to be adversely affected". It is also one of the risk factors, together with hazard ("The potential occurrence of a natural or human-induced physical event or trend that may cause loss of life, injury, or other health impacts, as well as damage and loss to property, infrastructure, livelihoods, service provision, ecosystems and environmental resources"; IPCC, 2019) and exposure ("The presence of people; livelihoods; species or ecosystems; environmental functions, services, and resources; infrastructure, or economic, social, or cultural assets in places and settings that could be adversely affected"; IPCC, 2019). In the context of climate change, "risks result from dynamic interactions between climate-related hazards with the exposure and vulnerability of the affected human or ecological system to the hazards" (IPCC, 2019). In this study we focus on the vulnerability of the shore to climate-related hazards, such as sea level rise or storms. Vulnerability can be divided itself in two components: susceptibility to harm and adaptability (i.e., the capacity of humans and ecosystems to cope and adapt). According to the definition above-mentioned, exposure can also be considered as a factor of vulnerability. A few studies already used a combination of factors in order to assess the vulnerability of the shore through a vulnerability index: physical, dynamic, or geomorphological factors (e.g., Peña-Alonso et al., 2017; Mathew et al., 2020), biological or ecological factors (e.g., Williams et al., 2001; Hereher, 2016), anthropogenic or socio-economic factors (e.g., Hereher, 2016; Mathew et al., 2020), climatological factors (Gornitz et al., 1994). In the latter case, climatological factors assess the potential hazard. The study from Gornitz et al. (1994) therefore does not only assess vulnerability, but the risk as a whole. The methods used ranged from analysing old and recent maps to using airborne and spaceborne imagery, databases, numerical models, and direct observations on the ground (e.g., Dune Vulnerability Index from García-Mora et al., 2001 and Williams et al., 2001; Coastal Vulnerability Index from Bagdanavičiūtė et al., 2015 and Hereher, 2016; Beach Vulnerability Index from Cazes-Duvat, 2001 and Alexandrakis and Poulos, 2014; Geomorphological Vulnerability Index from Peña-Alonso et al., 2017; Total Vulnerability Index from Mathew et al., 2020). Relevant criteria and tools for vulnerability assessment were adapted from these studies to create a new multidisciplinary index adapted to the case study of the island of Mayotte.

Coastal urbanisation is a worldwide trend (Cooper and Jackson, 2019) and also impacts the island of Mayotte with its recent demographic increase and socio-economic development. This study therefore had two main objectives: i) quantify the evolution of the typology and position of the shoreline of Mayotte since 1950; ii) identify which portions of the shoreline are particularly vulnerable and why, through the development of a multidisciplinary vulnerability index. Specifically, the study aims at applying the tools of shoreline evolution analysis and vulnerability assessment to the case of Mayotte. Aerial photographs of Mayotte since 1950 are available, allowing to study the shoreline evolution over several decades using high spatial resolution aerial photographs (Jeanson et al., 2019). The digitisation of the whole shoreline of Grande Terre at this scale since 1950 had never been done before, this is therefore the first research work to carry out an inventory of Mayotte's shoreline on the scale of the entire island and to suggest safeguard plans to be put in place. The first hypothesis of this study is that urbanisation and erosion of Mayotte's shoreline increase with time, following worldwide trends. The second hypothesis of this study is that coastal urbanisation increases the vulnerability of beaches. A multidisciplinary vulnerability index was developed to compare the vulnerability of several coastal sites depending on several factors (morpho-dynamic factors, protection by natural ecosystems, anthropogenic pressure). The innovative concept of this vulnerability index is its multidisciplinarity and thus adaptability to any field and context depending on the chosen criteria. Wider application of this index would allow coastal managers to select key coastal sites on which to undertake conservation and/or restoration actions.

## 2. Materials and methods

### 2.1. Study site: Mayotte

Mayotte is a French overseas department which is part of the Comoros volcanic archipelago in the Indian Ocean (12°50' S, 45°08' E) (Fig. 1). Mayotte has a tropical climate including a wet season with monsoon winds from North/North-West (during austral summer from December to March) and a dry season with stronger trade winds from the South/South-East (during austral winter from June to September) separated by two short shoulder seasons (Météo-France, 2021). These seasonal changes have a strong influence on the shoreline structure and dynamics (Jeanson et al., 2013, 2019). The different periods of erosion through time formed the current topography of the island, with a steep topography and pocket beaches between volcanic headlands (Nougier et al., 1986). The island is surrounded by a fringing reef, a lagoon, and a barrier reef. The specificities of the island are the lagoon, which is one of the widest and richest in the Indian Ocean (more than 1,000 km²), and the double barrier reef in the South-West (Masse et al., 1989; Jeanson, 2009; Leone et al., 2014; Chevalier et al., 2017). Coral reefs influence the hydrodynamics along the coast and play a protective role for the shore by decreasing the energy of waves and oceanic currents, depending on the structure of the reef (Jeanson et al., 2013). Tides in Mayotte are semi-diurnal and the tidal range is mesotidal (with a mean spring range of 3.20 m). Tide currents are therefore the main currents in the lagoon, and the oceanic currents have a less important role (Idier et al., 2008; Chevalier et al., 2017). The volcanic and tropical context of Mayotte together with the presence of large reefs, a lagoon, and associated hydrodynamic context lead to a high shoreline morphological diversity, suitable to host many different habitats and a high faunal biodiversity. The rugged coast extends along 240 km for Grande Terre and 25 km for Petite Terre (De La Torre and Aubie, 2003), with mainly cliffs interrupted by sandy or muddy bays where mangroves grow (Jeanson, 2009) (Fig. 1).

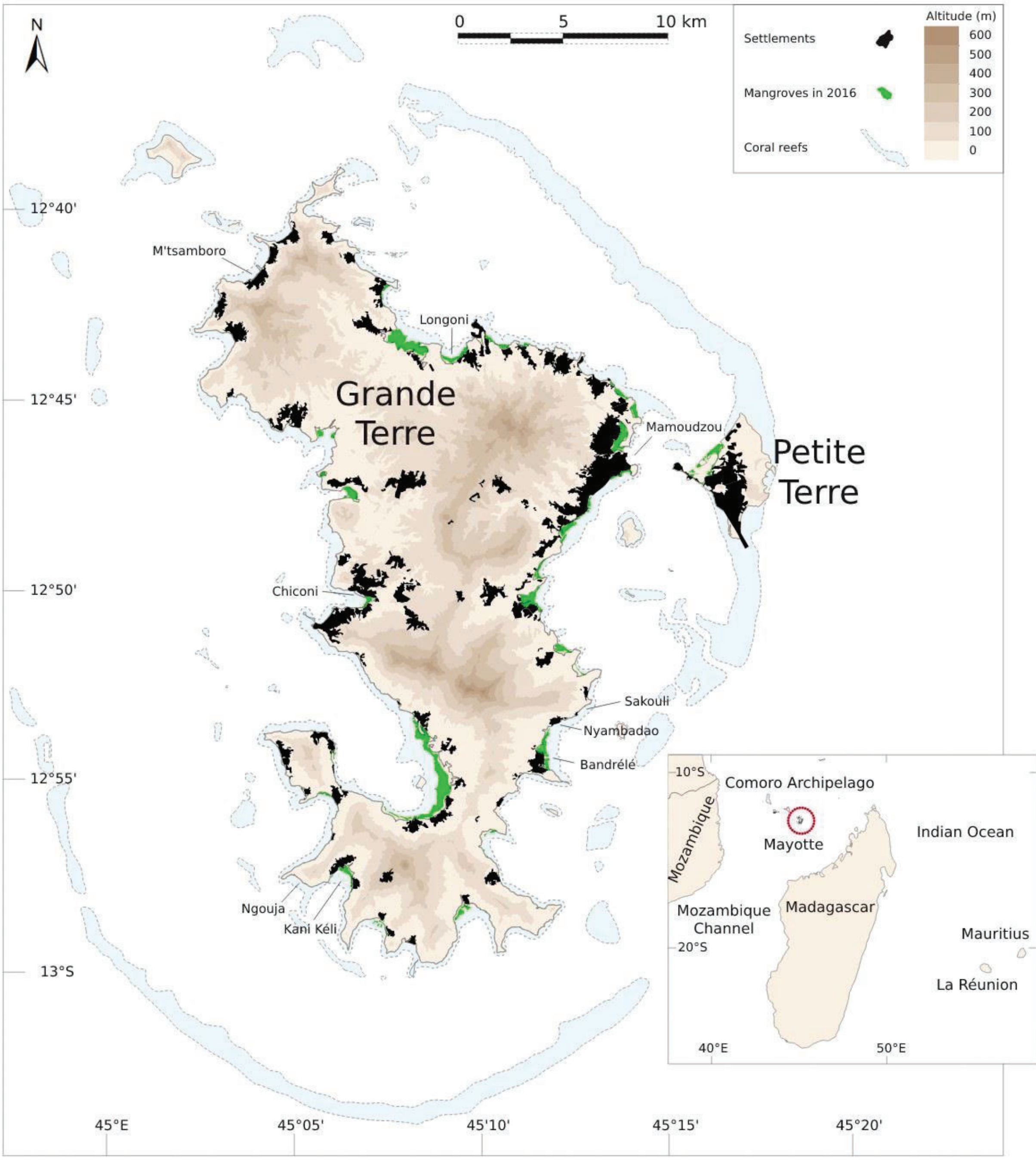


*Figure 1: Location of Mayotte Island, Indian Ocean (adapted from Jeanson et al., 2019).*

Mayotte is a French territory since 1841 and became the 101st French department in 2011. 256,500 inhabitants lived in Mayotte in 2017 (INSEE, 2017) and the population is very young. In 2017, more than half of the inhabitants were under 18 years old and the mean age was 23 years old. By comparison, the mean age in metropolitan France is 43 years old. Only one third of people in age of working in Mayotte have a job. This low employment can be explained by the poorly developed tourism and market sectors (agriculture, construction, industry, commerce, and other services). The non-market sector is more developed with many people working in public administration, education, health care and social actions. The buildings are traditionally organised in villages, with a mosque in the center, as the main religion in Mayotte is Islam. The territory is divided in 17 districts. The main urban pole is the axis Mamoudzou-Dzaoudzi, which are the principal towns on Grande Terre and Petite Terre, respectively. This urban pole includes the main infrastructures of the island (e.g., harbour, airport, prefecture, and hospital) and an industrial zone, condensing the main activities and the car traffic in this area. Grande Terre and Petite Terre are linked by a barge that travels from one island to the other on a regular basis every day. Many households live in precarious situations, with 40% of houses still made of sheet metal in 2017, 29% do not have access to running water, and 10% do not have access to electricity. However, living conditions improved since the 2000s (80% of houses did not have access to running water in 1997), but mainly for people living in permanent buildings. Over the course of 20 years, the population and habitations doubled, going from 130,000 inhabitants and 30,000 habitations in 1997 to 256,500 inhabitants and 63,100 principal residences in 2017 (INSEE, 2017).

This study includes several analyses of Mayotte's shoreline at different scales. As aerial photographs were available for the entire main island of Mayotte, Grande Terre, the analysis of changes in the shoreline category (rocky shore, beach, mangrove, urbanised shoreline) over time was done for the whole island. For practical reasons of software limitations and time available, the analysis of changes in the shoreline position over time was done only for twelve sites (three from each of the four categories, trying to be representative of what can be observed along all the island despite the practical constraints). The assessment of the criteria used in the development of the multidisciplinary vulnerability index requiring more fieldwork, the application of this index was done in only four sites to compare beaches with different local conditions.

### 2.2. Analysis of shoreline evolution based on aerial photographs

To characterise the shoreline evolution of Mayotte, a time series of aerial photographs of the main island of Mayotte (Grande Terre) was used: 1950, 1969, 1989, 2008, and 2016. Photographs from 2008 and 2016 were assembled and processed (orthorectified and georeferenced) by the French National Geographic Institude (IGN). Photographs from 1950, 1969, and 1989 were downloaded from the IGN website (https://remonterletemps.ign.fr/), cropped on XnConvert, assembled on Agisoft Metashape 1.7.1. (Professional Edition), and georeferenced in RGM04 (the local reference system of Mayotte) on ArcGIS 10.8.1 using the aerial photograph from 2016 as reference (following a method similar to Duvat and Pillet, 2017).

Based on the aerial photographs, the shoreline was manually traced at a scale of 1:2,000 in QGIS along all the coast. The shoreline was defined as the seaward limit of vegetation in natural areas and the seaward limit of human construction in urbanised areas as per previous studies (Duvat and Pillet, 2017; Collin et al., 2018). Three natural areas were distinguished: rocky shore, beach and mangrove. Urbanised areas were represented as a single category: urbanised shoreline. The choice of these categories relies on previous studies (De La Torre & Aubie, 2003; Madi Moussa et al., 2019) and on the capacity to discern them on aerial photographs.

Limitation of the software used does not allow to analyse the historical change of shoreline's position for the whole island at once. For practical reasons, it was therefore decided to select three sites from each category (rocky shore, beach, mangrove, and urbanised shoreline) along Mayotte's coast in order to try to obtain representative results for the whole island. The evolution of the position of the shoreline in each site was assessed by calculating the Net Shoreline Movement (NSM) and End Point Rate (EPR). The NSM was the distance between the oldest and the most recent shoreline (1950 and 2016, respectively). The EPR was calculated by dividing the NSM by the time elapsed between the oldest and the most recent shoreline (66 years). To do so, a module in ArcGIS was used: Digital Shoreline Analysis System version 5 (DSAS v5; Oyedotun, 2014). To calculate the uncertainty on the shoreline position, three sources of error needed to be taken into account: the spatial resolution of the photograph ($U_{res}$), the uncertainty from the georeferencing process (provided by the forward error of the ground control points on ArcGIS) ($U_{geo}$), and the uncertainty from shoreline tracing inaccuracies (estimated to be two meters for each date, because of the scale used during the tracing process: 1:2,000) ($U_{tra}$) (Table 1). Equation 1 from Hapke et al. (2011) allowed to combine these sources of error to obtain the uncertainty of the shoreline's position for each year ($U_{tot}$). Equation 2 from Hapke et al. (2011) was used to estimate the uncertainty of the rate in shoreline position change ($U_r$) between pairs of years. Between 1950 and 2016, the calculated shoreline change rate uncertainty ($U_r$) was of 0.08 m.y$^{-1}$.

$$U_{tot} = \sqrt{U_{res}^2 + U_{geo}^2 + U_{tra}^2} \quad \text{(Equation 1)} \qquad U_r = \frac{\sqrt{U_{tot,year1}^2 + U_{tot,year2}^2}}{year_2 - year_1} \quad \text{(Equation 2)}$$

*Table 1: Sources of uncertainty and total uncertainty for aerial photographs from 1950, 1969, 1989, 2008, and 2016.*

| | **Spatial resolution ($U_{res}$) (m)** | **Georeferencing uncertainty ($U_{geo}$) (m)** | **Tracing uncertainty ($U_{tra}$) (m)** | **Total uncertainty ($U_{tot}$) (m)** |
|---|---|---|---|---|
| **1950** | 1 | 4.6 | 2 | 5.1 |
| **1969** | 1 | 8.0 | 2 | 8.3 |
| **1989** | 1 | 7.8 | 2 | 8.1 |
| **2008** | 0.5 | 0 | 2 | 2.1 |
| **2016** | 0.5 | 0 | 2 | 2.1 |

## 2.3. Multidisciplinary vulnerability index: case study on four beaches in Mayotte

### *2.3.1. Development of the index*

While analyses of aerial photographs to assess Mayotte's shoreline evolution were done on the whole island of Grande Terre, the vulnerability assessment of Mayotte's shoreline in this study focused on four sites. Bandrélé, M'tsamboro, N'gouja, and Sakouli (Fig. 1) are representative sites for fringing reef beaches in Mayotte. The comparison of sandy shores with different levels of urbanisation allows to assess the impact of urbanisation on beach vulnerability, taking into account the local conditions. M'tsamboro is the most urbanised site, with a village directly behind the beach, and a wall defining the shoreline. In Bandrélé, there is a mangrove at the back of the beach, creating a buffer zone between the village and the beach. Sakouli and N'gouja are both more natural sites with mainly natural shoreline with vegetation and only a few hotels and restaurants at the back of the beach. The main difference between these two last sites is that N'gouja is a protected area, and it is therefore forbidden to fish there.

The method chosen to assess the vulnerability was the development of an index inspired by the coastal vulnerability index from Hereher (2016), and completed by other studies on coastal or beach vulnerability (Bodéré et al., 1991; Gornitz et al., 1994; Cazes-Duvat, 2001; García-Mora et al., 2001; Williams et al., 2001; Jeanson, 2004; Alexandrakis and Poulos, 2014; Peña-Alonso et al., 2017; Ruol et al., 2018; Mathew et al., 2020). The criteria used to assess the vulnerability (through susceptibility, adaptability, or exposure) of the beaches were chosen to be relevant based on the specific characters of the study area and were gathered in sub-indexes by field: morpho-dynamic, ecological and anthropogenic. The morpho-dynamic index and the anthropogenic index were based on 8 criteria with equal weights (Table 2). Weighting coefficient were not given to these criteria because the global level of vulnerability results from the combination of these criteria and not from each one individually (Cazes-Duvat, 2001). The ecological index was based on 11 criteria, with lower weights for interlinked criteria, giving a maximum score of 6 (Table 2). Each criterion was scored from 0 (condition linked to a low vulnerability) to 1 (condition linked to heightened vulnerability). For each site and each index, all the criteria were summed according to their weights and divided by the maximum score (8 for morpho-dynamic and anthropogenic indexes, 6 for ecological index) to obtain an index between 0 (minimum vulnerability) and 1 (maximum vulnerability). A global multidisciplinary vulnerability index ranging from 0 (minimum vulnerability) to 1 (maximum vulnerability) was calculated as the average of the three sub-indexes. No weighting coefficient were given to the sub-indexes because the global level of vulnerability results from the combination of these sub-indexes and not from each one individually (Cazes-Duvat, 2001). This method of use of a checklist of criteria to assess the feature of a site is originally based on the works from Bodéré et al. (1991) and Gornitz et al. (1994), and was already used and improved in several researches regarding coastal or beach vulnerability (e.g., Cazes-Duvat, 2001; García-Mora et al., 2001; Williams et al., 2001; Jeanson, 2004; Alexandrakis and Poulos, 2014; Hereher, 2016; Peña-Alonso et al., 2017; Ruol et al., 2018; Mathew et al., 2020) that were consulted in the development of our index.

### 2.3.2. Data acquisition

Most criteria were determined through punctual field observations on the four selected sites (Bandrélé, M'tsmaboro, N'gouja, and Sakouli) from March to July 2021. Some were also measured or calculated based on aerial photographs, and on data gathered in the field. Thus, topographic profiles were carried out with a Global Navigation Satellite System with Real Time Kinematic (GNSS RTK Trimble R8s). These profiles are done by taking the three-dimensional position of points a few meters apart along a line going from the shoreline to the fore-reef of the fringing reef at low tide, in the middle of the beach. Topographic profiles were used to determine two criteria: beach slope and beach width (Table 2). Pictures were taken at an altitude of 110 m (set to match the legal regulations and the practical constraints, i.e., the ratio between battery available and resolution needed) with an unmanned aerial vehicle (UAV) Dji Phantom 4 pro with a 20 megapixels sensor to cover the entire area of the beach with an overlapping of 80% in X and 75% in Y, from the shoreline to the fore-reef of the fringing reef. Orthophotos resulting from treatment of UAV pictures using Agisoft Metashape 1.7.1. (Professional Edition) were used to determine two criteria: width of the fringing reef and of the beach (Table 2).

*Table 2: Criteria used in the three sub-indexes on which is based the vulnerability index: morpho-dynamic index, ecological index, and anthropogenic index, with the method used to determine them, justification for the choice, and associated scores and weights. Criteria were determined qualitatively or quantitatively according to the data available. Results for each site and each criteria are provided in italic (BD: Bandrélé; MT: M'tsamboro; NG: N'gouja; SK: Sakouli). For each site, all the criteria were summed and divided by the maximum scores to obtain an index between 0 (minimum vulnerability) and 1 (maximum vulnerability). The thresholds between the scores were chosen in order to have a linear relation between the (rounded) smallest and highest values. The vulnerability index resulting from the combination of the three sub-indexes (morpho-dynamic, ecological, and anthropogenic) therefore reflects the relative vulnerability of the four sites, not an absolute vulnerability.*

| MORPHO-DYNAMIC INDEX | | | | | | | | |
|---|---|---|---|---|---|---|---|---|
| **Criteria** | **Determination of the criteria** | **Justification for the choice of criteria** | **Weight** | **Scores** | | | | |
| | | | | **0** | **0.25** | **0.5** | **0.75** | **1** |
| Presence of intertidal sand bars | Observation on the field | Intertidal sand bars represent a source of sediments, increasing the sediments budget and therefore the adaptability of the beach (Cohn et al., 2015) | 1 | Yes<br>*BD* | | | | No<br>*MT*<br>*NG*<br>*SK* |
| Texture of sediments | Estimation from observation on the field | Sediments texture is an indicator of the beach's capacity to cope with incident waves, with fine sediments being the most susceptible to transport, and therefore increasing the susceptibility of the beach (García-Mora et al., 2001; Williams et al., 2001; Alexandrakis and Poulos, 2014; Bagdanavičiūtė et al., 2015; Peña-Alonso et al., 2017) | 1 | Coarse sand | | Medium sand<br>*BD*<br>*MT*<br>*NG*<br>*SK* | | Fine sand |
| Beach slope (%) | Calculation on topographic profiles between the shoreline and the break in slope using Profiler 3.2 module in Excel | A steeper slope increases the susceptibility of the beach (Cazes-Duvat, 2001; Williams et al., 2001; Alexandrakis and Poulos, 2014) | 1 | ≤ 2<br>*BD* | 2 < X ≤ 4 | 4 < X ≤ 6 | 6 < X ≤ 8<br>*MT*<br>*SK* | > 8<br>*NG* |
| Beach width (m) | Measurements on drone pictures in | The width of the beach influences the | 1 | > 72<br>*SK* | 64 < X ≤ 72<br>*BD* | 56 < X < 64 | 48 < X ≤ 56<br>*NG* | ≤ 48<br>*MT* |

| | | | | | | | | |
|---|---|---|---|---|---|---|---|---|
| | ArcGIS via the estimation of the position of the break in slope on the topographic profiles | availability of sediments on the beach. Wider beaches having larger surface exposed to waves, the intensity of this agent on the beach is decreased, promoting the deposition of sediments and decreasing the susceptibility of the beach (Bodéré et al., 1991; Cazes-Duvat, 2001; García-Mora et al., 2001; Williams et al., 2001; Alexandrakis and Poulos, 2014; Bagdanavičiūtė et al., 2015; Peña-Alonso et al., 2017; Ruol et al., 2018) | | | | | | |
| Sedimentary evolution between 1950 and 2016 | Calculation on aerial photographs using DSAS module in ArcGIS | The shoreline erosion/accretion on several previous decades indicates the past history of sedimentary evolution of the shoreline and offers a basis for future projections of shoreline response to sea level rise. Past erosion trend therefore shows a lower adaptability of the beach (Bodéré et al., | 1 | Accretion<br>*BD* | | Stability<br>*MT*<br>*NG*<br>*SK* | | Erosion |

| | | | | | | | | |
|---|---|---|---|---|---|---|---|---|
| | | 1991; Gornitz et al., 1994; Cazes-Duvat, 2001; Williams et al., 2001; Bagdanavičiūtė et al., 2015; Peña-Alonso et al., 2017) | | | | | | |
| Supply in terrigenous sediments | Estimation from the calculation of the surface of the catchment area above each beach on ArcGIS | Higher supply in terrigeneous sediments increases the adaptability of the beach (Alexandrakis and Poulos, 2014) | 1 | Important<br>*BD* | | Moderate<br>*MT*<br>*SK* | | Low<br>*NG* |
| Exposition to waves and swell | Observation on the field | More exposed beaches have a higher exposure and susceptibility (García-Mora et al., 2001; Peña-Alonso et al., 2017) | 1 | Sheltered | | | *BD*<br>*MT*<br>*NG*<br>*SK* | Exposed |
| Tidal range (m) | Theorical values | Large tidal range is associated with strong tidal currents that can transport unconsolidated sediments, with a wide intertidal zone susceptible to episodic flooding and penetration of saline water following sea level rise and/or storm surges and thus potentially impacting the wetland ecology. Therefore, macrotidal coasts are more vulnerable than those with lower | 1 | Microtidal<br>(≤ 2) | | Mesotidal<br>(2 < X ≤ 4)<br>*BD*<br>*MT*<br>*NG*<br>*SK* | | Macrotidal<br>(> 4) |

| | | | | | | | | |
|---|---|---|---|---|---|---|---|---|
| | | tide ranges (Gornitz et al., 1994; Williams et al., 2001; Peña-Alonso et al., 2017) | | | | | | |
| **ECOLOGICAL INDEX** | | | | | | | | |
| **Criteria** | **Determination of the criteria** | **Justification for the choice of criteria** | **Weight** | **Scores** | | | | |
| | | | | **0** | **0.25** | **0.5** | **0.75** | **1** |
| Presence of associated ecosystem protecting the coast: mangrove | Observation on the field | Mangroves play a protective role for the shore (e.g., dissipation of wave energy and sediment stabilisation), decreasing its susceptibility (Jeanson et al., 2014; Spalding et al., 2014; Guannel et al., 2016; Narayan et al., 2016; Powell et al., 2019) | 1 | Yes<br>*BD* | | | | No<br>*MT*<br>*NG*<br>*SK* |
| Presence of associated ecosystem protecting the coast: seagrass bed | Observation on the field | Seagrass beds play a protective role for the shore (e.g., dissipation of wave energy and sediment stabilisation), decreasing its susceptibility (Ondiviela et al., 2014; Spalding et al., 2014; Guannel et al., 2016; Narayan et al., 2016) | 0.5 | Yes<br>*BD*<br>*MT*<br>*NG*<br>*SK* | | | | No |
| Density of seagrass bed | Qualitative estimation based on visual observation at low tide | Higher density enhances the protective role of seagrass bed (e.g., dissipation of wave energy and sediment stabilisation), therefore decreasing | 0.5 | Very high | High | Moderate<br>*NG* | Low<br>*MT*<br>*SK* | Very low<br>*BD* |

| | | | | | | | | |
|---|---|---|---|---|---|---|---|---|
| | | exposure and susceptibility of the shore (Ondiviela et al., 2014) | | | | | | |
| Presence of associated ecosystem protecting the coast: fringing reef | Observation on the field and on aerial photographs | Fringing reefs play a protective role for the shore (e.g., dissipation of wave energy and sediment provision), decreasing its susceptibility (Spalding et al., 2014; Guannel et al., 2016; Narayan et al., 2016; Powell et al., 2019) | 0.75 | Yes<br>*BD*<br>*MT*<br>*NG*<br>*SK* | | | | No |
| Distance between the shoreline and the reef front of the fringing reef (m) | Measurements of the distance between the shoreline and the reef front of the fringing reef in the middle of the beach on drone pictures in ArcGIS. | Beaches can be separated in 3 categories: open beaches least vulnerable to erosion, beaches at a distance of the reef front between 150 and 500 m very vulnerable to erosion, and beaches at a distance of the reef front between 500 and 3000 m with intermediate vulnerability (Cazes-Duvat, 2001) | 0.25 | > 3000 (open beach) | | 500 < X ≤ 3000<br>*BD* | | ≤ 500<br>*MT*<br>*NG*<br>*SK* |
| Presence of associated ecosystem protecting the coast: barrier reef | Observation on aerial photographs | Barrier reefs play a protective role for the shore (e.g., dissipation of wave energy and breaking of offshore waves), decreasing its susceptibility (Spalding et al., | 0.5 | Yes (double barrier)<br>*NG* | Yes (continuous barrier) | Yes (discontinuous barrier)<br>*BD*<br>*MT*<br>*SK* | | No |

| | | | | | | | | |
|---|---|---|---|---|---|---|---|---|
| | | 2014; Guannel et al., 2016; Narayan et al., 2016; Powell et al., 2019) | | | | | | |
| Distance between the shoreline and the barrier reef (lagoon width) (km) | Measurements on aerial photographs in ArcGIS | The higher the distance between the shore and the barrier reef is, the more wind-waves can be generated and increase with wind, increasing the susceptibility of the shore (Gallop et al., 2014) | 0.25 | ≤ 2 | 2 < X ≤ 4 | 4 < X ≤ 6 *BD* *SK* | 6 < X ≤ 8 | > 8 *MT* *NG* |
| Width of the barrier reef (m) | Measurements on aerial photographs in ArcGIS | The protective role of the barrier reef (dissipation of wave energy) increases with the reef width, therefore decreasing exposure and susceptibility of the shore (Kench and Brander, 2006; Jeanson, 2009; Spalding et al., 2014; Narayan et al., 2016) | 0.25 | > 1700 *MT* | 1400 < X ≤ 1700 | 1100 < X ≤ 1400 | 800 < X ≤ 1100 *BD* *NG* *SK* | ≤ 800 |
| Wrack | Observation on the field | Wrack plays a protective role for the shore by attenuating wave energy and trapping sediments, therefore decreasing susceptibility of the beach (Bodéré et al., 1991; Robbe et al., 2021) | 1 | Important | | Moderate | | Low *BD* *MT* *NG* *SK* |
| High vegetation | Observation on the field | Coastal vegetation plays | 0.5 | Important *BD* | *NG* *SK* | Moderate | *MT* | None |

| | | | | | | | | |
|---|---|---|---|---|---|---|---|---|
| (i.e., trees and shrubs) in upper beach | | a protective role against erosion by trapping and stabilising coastal sediments, therefore decreasing the susceptibility of the beach (Bodéré et al., 1991; Williams et al., 2001; Lee et al., 2020) | | | | | | |
| Low and creeping vegetation (i.e., herbaceous plants and vines) in upper beach | Observation on the field | Coastal vegetation plays a protective role against erosion by trapping and stabilising coastal sediments, therefore decreasing the susceptibility of the beach (Bodéré et al., 1991; Lee et al., 2020) | 0.5 | Important | | Moderate<br>*SK* | *MT*<br>*NG* | None<br>*BD* |
| **ANTHROPOGENIC INDEX** | | | | | | | | |
| **Criteria** | **Determination of the criteria** | **Justification for the choice of criteria** | **Weight** | **Scores** | | | | |
| | | | | **0** | **0.25** | **0.5** | **0.75** | **1** |
| Beach frequentation | Observation on the field | High beach frequentation alters geomorphology and equilibrium of the beaches, therefore increasing exposure and susceptibility, and decreasing natural adaptability of the beach (Bodéré et al., 1991; Simeone et al., 2012; Peña-Alonso et al., 2017) | 1 | Low<br>*BD* | | Moderate<br>*MT* | | High<br>*NG*<br>*SK* |

| | | | | | | | | |
|---|---|---|---|---|---|---|---|---|
| Reef flat frequentation | Observation on the field | Higher reef flat frequentation can damage the reef and decrease its protective role (e.g., dissipation of wave energy and sediment stabilisation), therefore increasing the susceptibility of the beach (Guannel et al., 2016; Powell et al., 2019) | 1 | Low<br>*NG* | *SK* | Moderate<br>*BD* | *MT* | High |
| Motorised vehicles on the beach | Observation on the field | Vehicles transit on the beach alters the equilibrium profiles of the beaches, and prevents plant from growing and acting as obstacles to sedimentary transport, therefore increasing exposure and susceptibility, and decreasing natural adaptability of the beach (Bodéré et al., 1991; Kindermann and Gormally, 2010; Peña-Alonso et al., 2017) | 1 | None<br>*BD*<br>*MT*<br>*NG*<br>*SK* | | Some | | A lot |
| Presence of coastal defences | Observation on the field | Hard coastal defences modify the limits of the beaches and alter coastal drift and the natural transport of the sediments (potentially causing | 1 | No<br>*BD*<br>*NG*<br>*SK* | | | | Yes<br>*MT* |

| | | | | | | | | |
|---|---|---|---|---|---|---|---|---|
| | | acceleration or displacement of erosion), increasing exposure and susceptibility, and decreasing natural adaptability of the beach (Cazes-Duvat, 2001; Nordstrom, 2004; Peña-Alonso et al., 2017) | | | | | | |
| Importance of urbanisation | Observation on the field | More urbanisation decreases the natural adaptability of the beach (Bodéré et al., 1991; Cazes-Duvat, 2001; García-Mora et al., 2001; Hereher, 2016; Peña-Alonso et al., 2017; Ruol et al., 2018) | 1 | Low | | Moderate<br>*NG*<br>*SK* | *BD* | High<br>*MT* |
| Boat anchoring | Observation on the field | Boats anchoring damages the protective ecosystems along the coast, decreases their protection, and therefore increases the susceptibility of the beach (Liu et al., 2021) | 1 | None | Low<br>*BD*<br>*NG*<br>*SK* | Moderate | | Important<br>MT |
| Waste water discharge near the coast | Observation on the field | Pollution from waste water discharge damages the health of protective ecosystems along the coast, decreases their protection and therefore | 1 | None | Low<br>*NG*<br>*SK* | Moderate | Important<br>*BD*<br>*MT* | Very important |

| | | | | | | | | |
|---|---|---|---|---|---|---|---|---|
| | | increases the susceptibility of the beach (Tuholske et al., 2021) | | | | | | |
| Sand mining | Observation on the field | Sand mining alters equilibrium of the beaches, therefore increasing exposure and susceptibility, and decreasing natural adaptability of the beach (Bodéré et al., 1991; Cazes-Duvat, 2001) | 1 | None<br>*NG*<br>*SK* | Low<br>*BD*<br>*MT* | Moderate | | Important |

# 3. Results

## 3.1. Characterisation of Mayotte's shoreline evolution

The changes between 1950 and 2016 of Grande Terre shoreline typology were limited, with a noticeable change only in terms of urbanised shoreline, increasing from 1% in 1950 to 6% in 2016 (Fig. 2 and 3). The percentage of beaches along the shoreline was stable across time, and the mangroves showed some variability between the years but an overall long-term stability in shoreline length occupied by mangroves (Fig. 3). Urbanisation was therefore mainly conducted on rocky shores, with the biggest change taking place between 1989 and 2008 (urbanised shoreline increasing from 3 to 6%, Fig. 2 and 3).

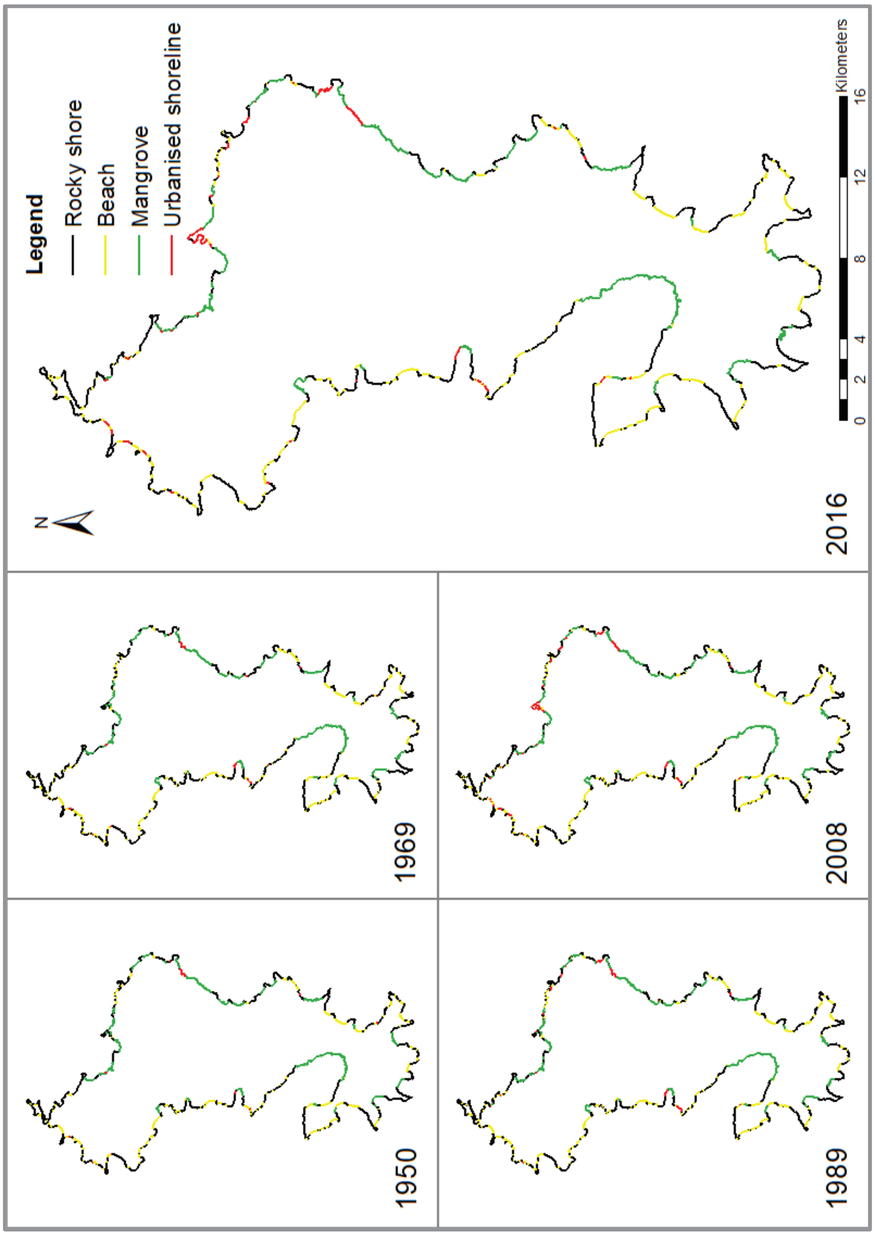


*Figure 2: Map of the shoreline classification of Grande Terre (the main island of Mayotte) in 1950, 1969, 1989, 2008, and 2016. Rocky shore in black, beach in yellow, mangrove in green, urbanised shoreline in red.*

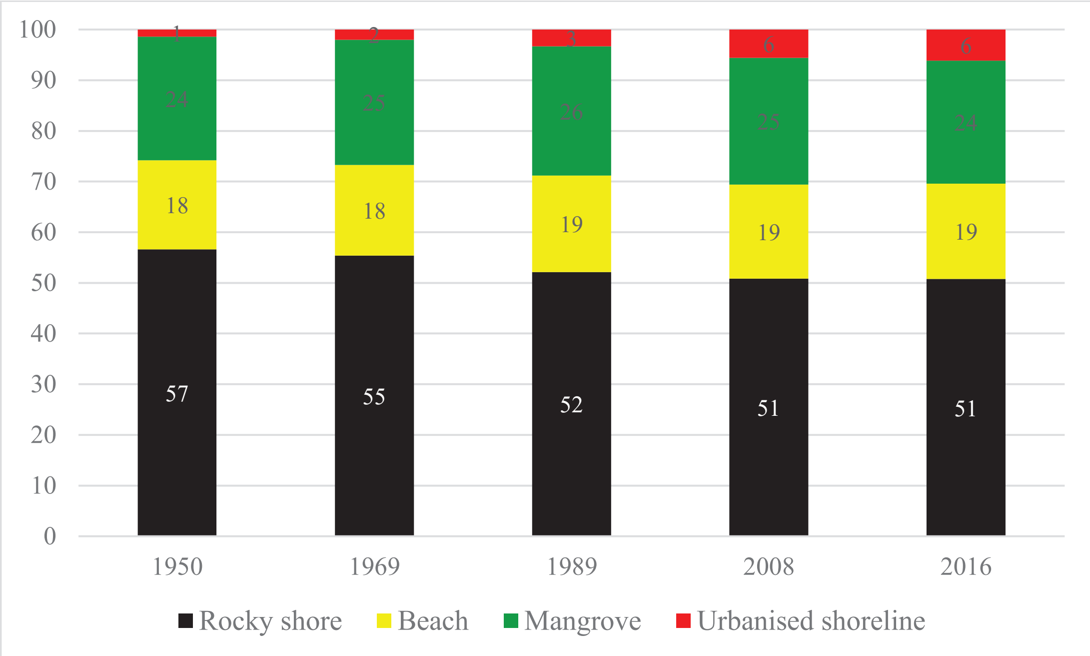


*Figure 3: Percentage of the shoreline as rocky shore, beach, mangrove and urbanised area in 1950, 1969, 1989, 2008, and 2016 on the main island of Mayotte (Grande Terre).*

The analysis of changes in the shoreline position between 1950 and 2016 (Fig. 4, 5, 6, and 7) (with a shoreline change rate uncertainty of 8 $cm.y^{-1}$) showed that the rocky shore did not display any change: between -5 ± 8 $cm.y^{-1}$ and 0 ± 8 $cm.y^{-1}$ (Fig. 4). The beaches were more dynamic environments: -2 ± 8 $cm.y^{-1}$ for M'tsamboro; -6 ± 8 $cm.y^{-1}$ for Sakouli; 10 ± 8 $cm.y^{-1}$ for N'gouja (Fig. 5). The mangroves were more dynamic on shorter terms with an accretion for Longoni (19 ± 8 $cm.y^{-1}$) and Bandrélé (27 ± 8 $cm.y^{-1}$) (Fig. 6). The third mangrove (Kani-Kéli) showed an overall stability with a change rate of -1 ± 8 $cm.y^{-1}$, although a trend of accretion in the northern section of the mangrove, and a trend of erosion in the eastern section of the mangrove emerged (Fig. 6). The most impressive changes were in urbanised areas: Mamoudzou with a change rate of 101 ± 8 $cm.y^{-1}$, and Chiconi with a change rate of 55 ± 8 $cm.y^{-1}$ (Fig. 7).

The trends that can be drawn from these results are therefore a stability of the rocky coasts; a slight variability between the beaches which are mostly stable or show slight accretion or erosion trends; a more marked variability of the mangroves which are mostly accreting or stable overall, but with sometimes erosion and accretion within the same mangrove depending on the section observed; and a result of considerable accretion for the large urban areas because of infrastructure building gaining ground at the expense of the sea (not marked for smaller villages). However, these trends should be taken with caution as they are based on only three sites in each category, and not on an analysis covering the whole island.

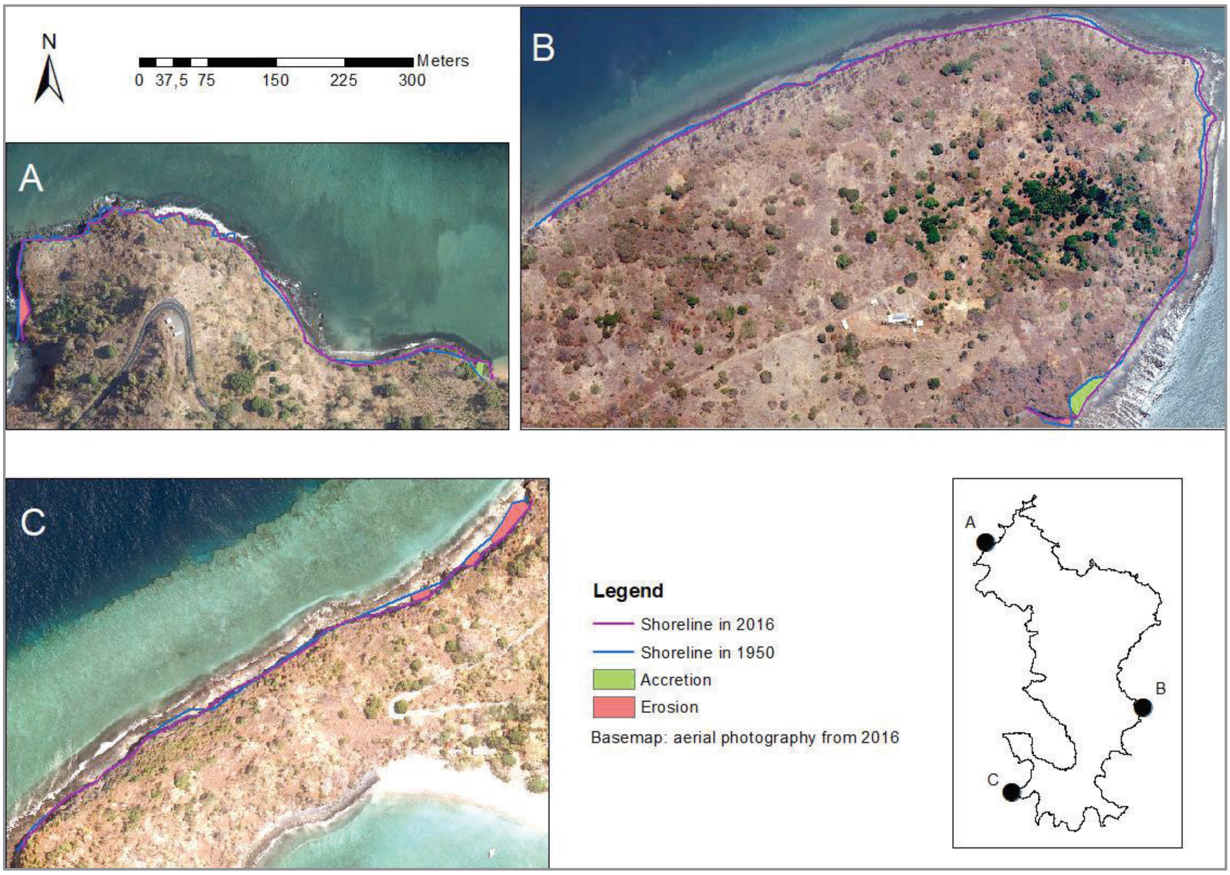


*Figure 4: Evolution of the position of the shoreline (rocky shore) between 1950 and 2016 in three locations: north-west with a mean shoreline movement of 0 m and a mean end point rate of 0 $m.y^{-1}$ (A), center-east with a mean shoreline movement of 0 m and a mean end point rate of 0 $m.y^{-1}$ (B), and south-west with a mean shoreline movement of -3 m and a mean end point rate of -0.05 $m.y^{-1}$ (C). The net shoreline movement (m) and end point rate ($m.y^{-1}$) are extracted from the DSAS module in ArcGIS 10.8.1.*

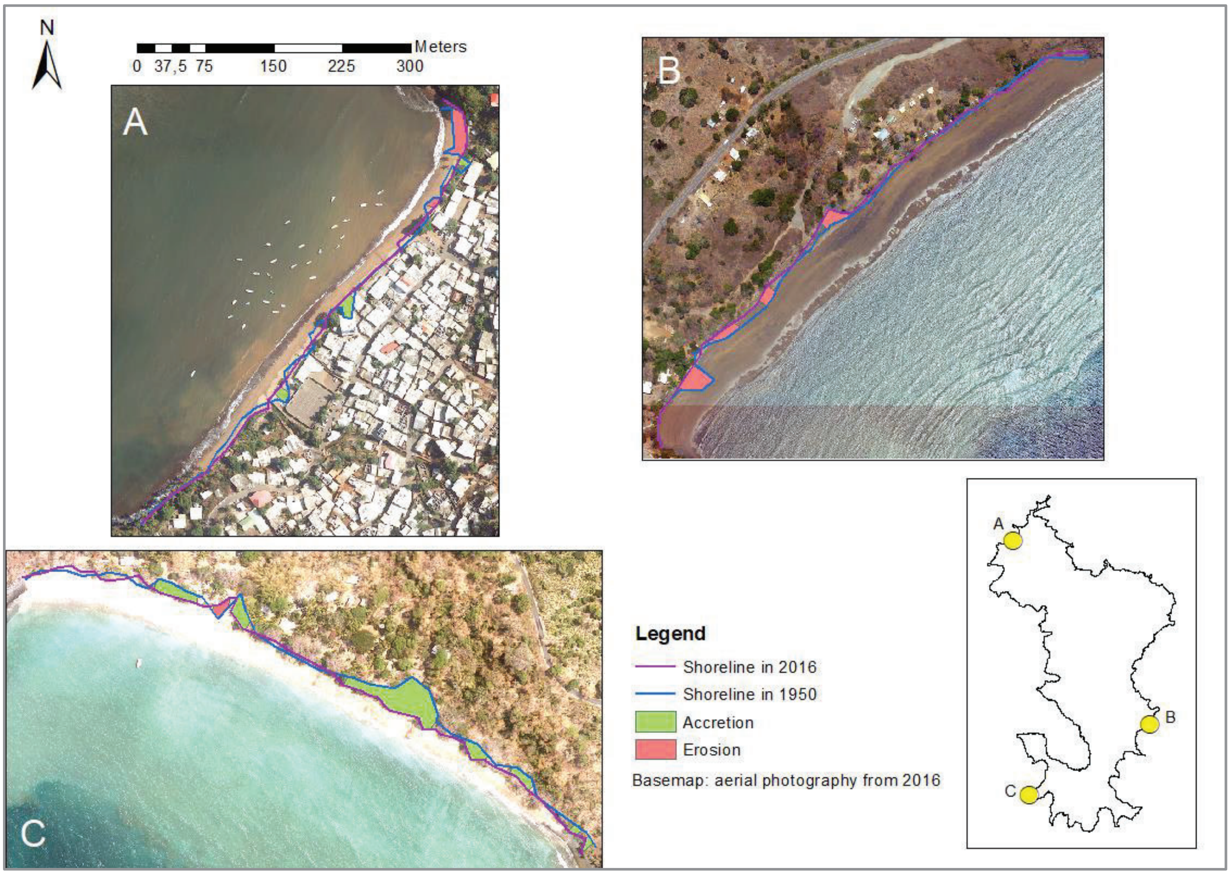


*Figure 5: Evolution of the position of the shoreline (beach) between 1950 and 2016 in three locations: M'tsamboro in the north-west with a mean shoreline movement of -2 m and a mean end point rate of -0.02 $m.y^{-1}$ (A), Sakouli in the center-east with a mean shoreline movement of -4 m and a mean end point rate of -0.06 $m.y^{-1}$ (B), and N'gouja in the south-west with a mean shoreline movement of 6 m and a mean end point rate of 0.10 $m.y^{-1}$ (C). The net shoreline movement (m) and end point rate ($m.y^{-1}$) are extracted from the DSAS module in ArcGIS 10.8.1.*

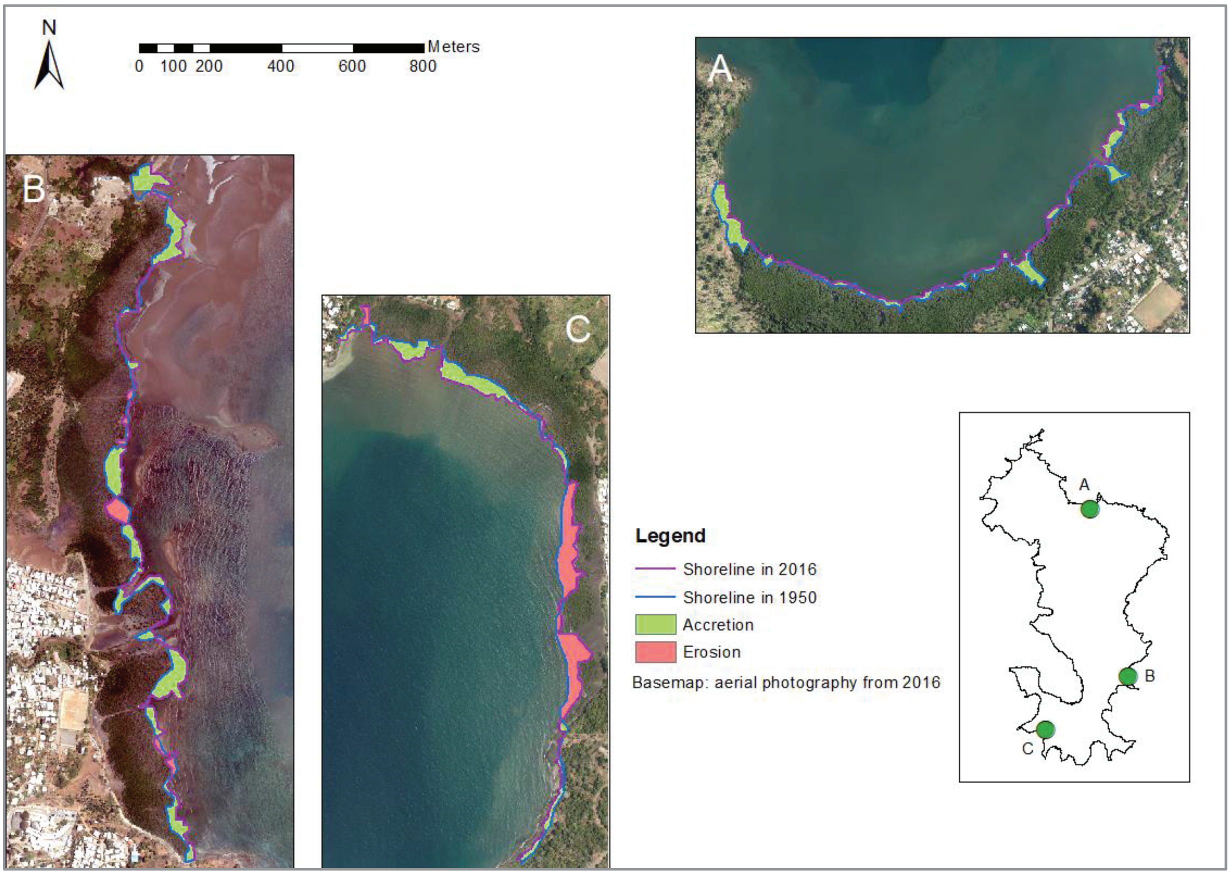


*Figure 6: Evolution of the position of the shoreline (mangrove) between 1950 and 2016 in three locations: the mangrove of Longoni in the north with a mean shoreline movement of 12 m and a mean end point rate of 0.19 m.y$^{-1}$ (A), the mangrove of Bandrélé in the center-east with a mean shoreline movement of 18 m and a mean end point rate of 0.27 m.y$^{-1}$ (B), and the mangrove of Kani-Kéli in the south with a mean shoreline movement of -1 m and a mean end point rate of -0.01 m.y$^{-1}$ (C). The net shoreline movement (m) and end point rate (m.y$^{-1}$) are extracted from the DSAS module in ArcGIS 10.8.1.*

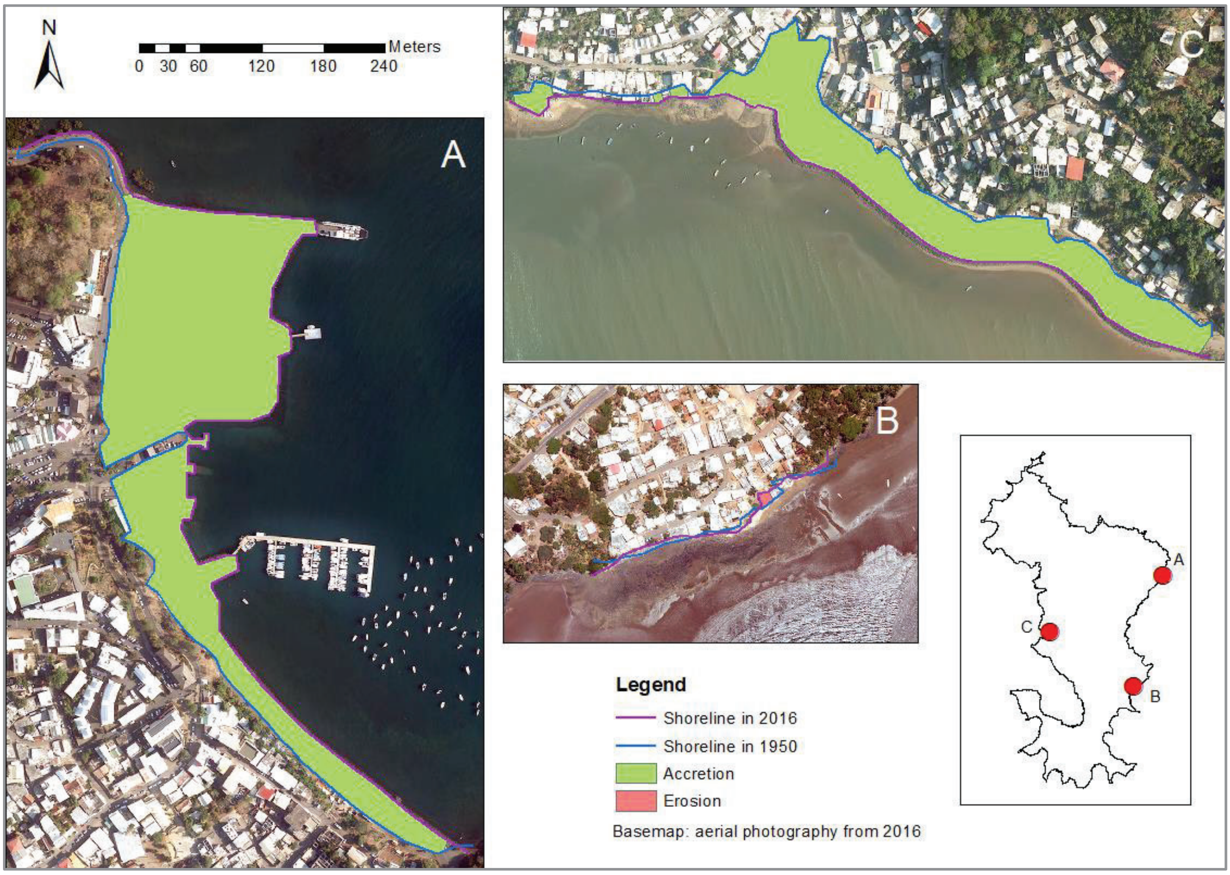


*Figure 7: Evolution of the position of the shoreline (urbanised shoreline) between 1950 and 2016 in three locations: Mamoudzou in the north-east with a mean shoreline movement of 66 m and a mean end point rate of 1.01 m.y$^{-1}$ (A), Nyambadao in the center-east with a mean shoreline movement of -1 m and a mean end point rate of -0.01 m.y$^{-1}$ (B), and Chiconi in the center-west with a mean shoreline movement of 36 m and a mean end point rate of 0.55 m.y$^{-1}$ (C). The net shoreline movement (m) and end point rate (m.y$^{-1}$) are extracted from the DSAS module in ArcGIS 10.8.1.*

### 3.2. Beach vulnerability index

The scores given to each site (BD for Bandrélé, MT for M'tsamboro, NG for N'gouja, and SK for Sakouli) for each criteria were presented in Table 2. The three sub-indexes and the multidisciplinary vulnerability index obtained after calculations were presented in Figure 8.

The morpho-dynamic index showed that Bandrélé had a low morpho-dynamic vulnerability (0.25) followed by Sakouli (0.56), and then by M'tsamboro (0.69) and N'gouja (0.75) (Fig. 8A). Bandrélé displayed the lowest ecological vulnerability (0.45) and M'tsamboro the highest (0.65), while N'gouja and Sakouli displayed intermediate values (0.57 and 0.59, respectively) (Fig. 8B). The vulnerability linked to anthropogenic pressures was higher in M'tsamboro (0.66) than in the three other sites (between 0.25 and 0.31) (Fig. 8C). Combining the three sub-indexes in a global multidisciplinary index allowed to discrimate the lowest vulnerability for Bandrélé (0.34, mainly linked to morpho-dynamic and ecological factors) and the highest for M'tsamboro (0.66, mainly linked to ecological and anthropogenic factors) (Fig. 8D). Sakouli and N'gouja displayed intermediate values of vulnerability (0.48 and 0.52, respectively) (Fig. 8D).

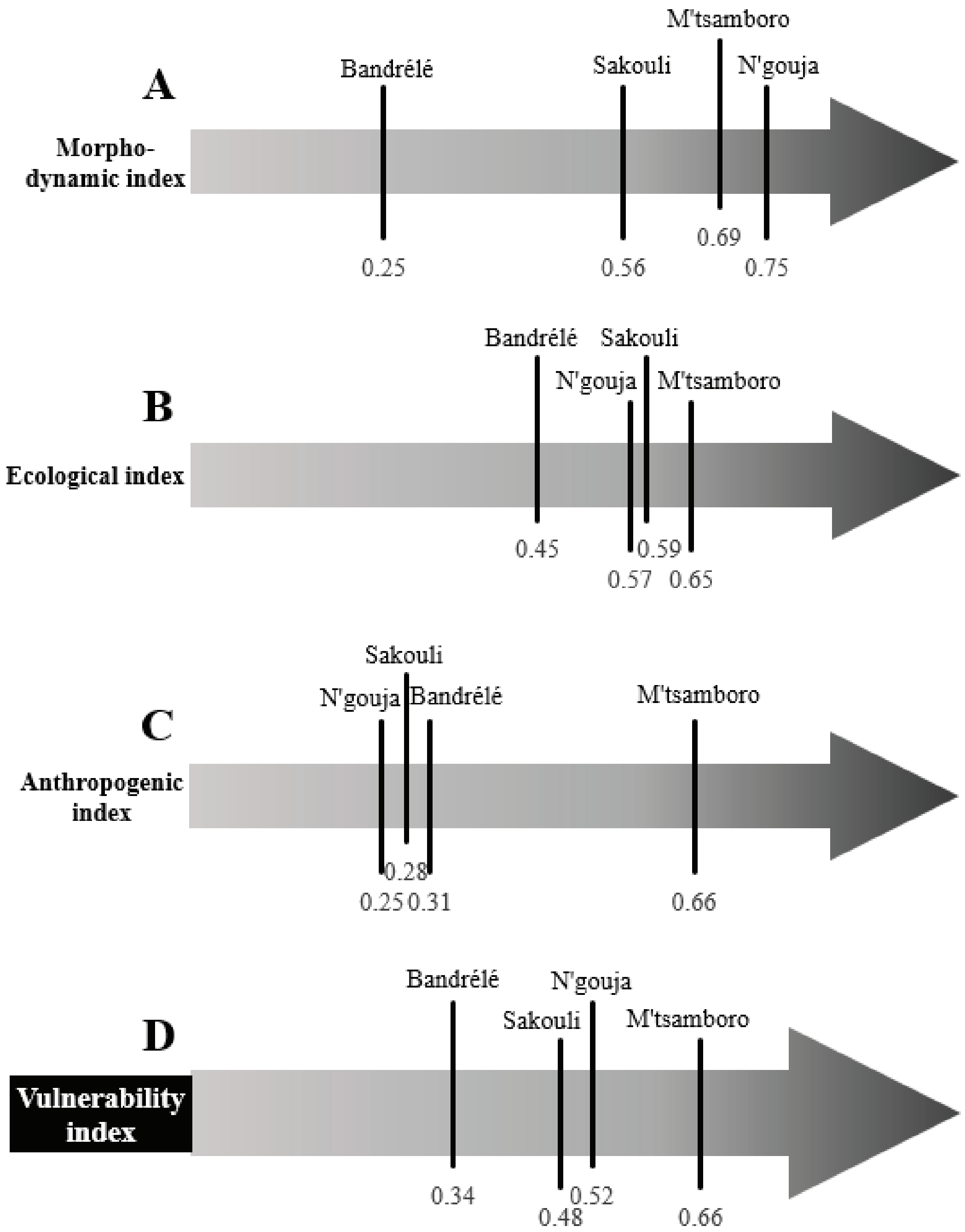


*Figure 8: Beach vulnerability index (D) of four beaches in Mayotte (Bandrélé, M'tsamboro, N'gouja, and Sakouli) and its three components: morpho-dynamic index (A), ecological index (B), and anthropogenic index (C). The left part of the arrows represents the minimum vulnerability (0), while the right part of the arrows represents the maximum vulnerability (1).*

# 4. Discussion

## 4.1. Characterisation of Mayotte's shoreline evolution

Artificialisation of Mayotte's shoreline is a reality, but remains limited nowadays (the urbanised shoreline increased from 1% in 1950 to 6% in 2016, Fig. 3) compared to the trends in other parts of France (e.g., metropolitan France, French West Indies, French Polynesia, La Réunion, etc.; Le Berre, 2017; Madi Moussa et al., 2019; Gairin et al., 2021; Giraud-Renard et al., 2022) and worldwide (Adger et al., 2005; Airoldi and Beck, 2007; Dugan et al., 2011; Gittman et al., 2016; Matić-Skoko et al., 2020). As an example, more than 50% of the land in coastal areas is urbanised in several European countries (Airoldi and Beck, 2007). Taking two examples of islands in other parts of the world, the urbanised shoreline increased from 4% in 1950 to 21% in 2017 in Guadeloupe (study on a part of the northern and southern shorelines; Giraud-Renard et al., 2022) and from 12% in 1955 to 61% in 2019 in Bora Bora (Gairin et al., 2021). This "delay" in shoreline urbanisation in Mayotte could be explained by several physical and socio-economic factors. Firstly, the high tidal range in Mayotte (3.20 m) makes it difficult to build directly on the shoreline and in the intertidal area (e.g., a high volume of material would be necessary to be able to build embankments that would not be flooded during high tide, tidal currents would put more pressure on infrastructure, etc.), and therefore narrows the space available for permanent human infrastructure. In Bora Bora and Guadeloupe, the tidal range is only 30-50 cm, making the land-water interface more attractive for constructions. The nature of the island of Mayotte, with its steep slopes, numerous rocky shores with cliffs, and no coastal plain, is also a factor explaining the low urbanisation on the shoreline. Moreover, the global development in Mayotte occurred recently, with an increasing demographic pressure lately (the population doubled in 20 years, going from 130,000 inhabitants in 1997 to 256,500 in 2017; INSEE, 2017). Thus, the main increase in shoreline urbanisation took place between 1989 and 2008 (from 3 to 6%, Fig. 3). This period coincides with a strengthening of ties between metropolitan France and Mayotte (notably as Mayotte became a French Territorial Collectivity in 1976, and a French department in 2011), improving socio-economic conditions and medical care (thus decreasing mortality) (Bernardie-Tahir and El-Mahaboubi, 2001). It is also a period of economic development with the construction of the deepwater port in Longoni in the 2000s and the development of the industrial area around Mamoudzou (Jeanson et al., 2019). The construction of habitations and roads often takes place near the sea, as the population concentrates there mainly because of the strong mountain slopes on the island and economic issues, but not systematically on the shoreline itself (Bernardie-Tahir and El-Mahaboubi, 2001; Jeanson et al., 2014). The percentage of urbanisation would therefore likely be much higher in a study focusing on a larger littoral fringe than the shoreline itself (viewed as a line and not an area in this study). Overall, as the majority of the shoreline is still natural, a sound management advice would be to put in place conservation measures to preserve this natural environment.

The shoreline was divided in four categories in this study: rocky (rocky shore, 51% in 2016), muddy (mangrove, 24% in 2016), sandy (beach, 19% in 2016), and artificial (urbanised shoreline, 6% in 2016) (Fig. 3). The changes over time from 1950 to 2016 were assessed for three sites of each category. None of the rocky shores showed any change in extent or position (Fig. 4), as they are the most stable environment. Only one of the beaches analysed showed an accretion of a few centimeters per year (N'gouja, Fig. 5). It is a tricky task to assess the evolution of beaches because of multiple special cases. Some beaches display erosion while others display accretion (e.g., terrigenous sediments inputs due to high soil erosion favour accretion of beaches) and hints of both phenomena can be seen within one beach (e.g., Fig. 5A and 5B), suggesting a succession of calm episodes favourable to sedimentation and punctual extreme events causing erosion. The beaches are dynamic environments at a seasonal scale, with long-shore (e.g., N'gouja) or cross-shore sand exchange movements changing direction each season. However, they appear relatively stable over several decades, suggesting that the coral reef environment protects them from losing sediments (Jeanson et al., 2013, 2019). There is more variability regarding the evolution of mangroves, with erosion or accretion trends depending on each mangrove, and even within the mangrove (e.g., mangrove of Kani-Kéli; Fig. 6). Mangroves on the west and south coast of the island display losses in extent over the sea, while on the north coast they show stability or a little prograding (Jeanson et al., 2014, 2019), suggesting that mangrove resilience depends on the morphodynamics and hydrodynamics of the reef, which vary around the island (Jeanson et al., 2013). Mangroves are constituted of living trees, and therefore evolve at a shorter-term than rocks or beaches. The evolution of mangroves also depends on local anthropogenic (e.g., cut of trees, urbanisation) and natural (e.g., silting, hydro-sedimentary processes) factors (Jeanson et al., 2014). However, in the current context of siltation in Mayotte, mangroves display a relative stability (Jeanson, 2009). The changes of the urbanised shoreline position are the most impressive, as modifications from anthropogenic origin are more drastic than natural ones. Some villages, like Nyambadao, do not have a big impact on the shoreline position, while others, like Chiconi and Mamoudzou, build walls and embankments, gaining ground at the expense of the sea (Fig. 7). Mamoudzou is a special example of urban development. It is the main city of Mayotte and the studied area is the main harbour which links Petite Terre (the island with the only airport of Mayotte) and Grande Terre (the main island of Mayotte). This strategic location can therefore explain the extent of artificialisation and thus the strong seaward change of the position of the shoreline: it is one of the main areas involved in the economy of the island (Jeanson et al., 2019).

The choice of three sites from each category of shoreline was done to try to obtain representative results for the entire island. However, the specific conditions and results for each site (mainly beaches, mangroves, and urbanised sites) do not allow to conclude that our results are a valid representation of the whole island's shoreline. A further study of the coastal sites of the entire island would be necessary to be able to obtain a representative conclusion for the whole island.

### 4.2. Beach vulnerability index

The vulnerability index is applied to four beaches along the coast of Mayotte, with different levels of urbanisation and local conditions. Among the four sites, the most urbanised site, M'tsamboro, displays the highest vulnerability, and Bandrélé the lowest, while Sakouli and N'gouja have intermediate vulnerability (Fig. 8). The three sub-indexes help to understand which factors play the main role in the assessment of the vulnerability. The presence of the mangrove in Bandrélé plays a role of protection of the coast, decreasing the vulnerability of the beach through ecological factors (Fig. 8B). Indeed, mangroves commonly play a role of buffer between the land and beach and trap sediments (Jeanson et al., 2014).

Morpho-dynamic factors also decrease the vulnerability of this site (Fig. 8A). In contrast, the more developed urbanisation in M'tsamboro increases its vulnerability, mainly through the anthropogenic sub-index (Fig. 8C) but also through the ecological sub-index (Fig. 8B), including because of the impact of urbanisation on ecosystems. The choice was made to study the vulnerability of the beaches. That is why Bandrélé is not considered as having high anthropogenic pressure despite having a village nearby: we consider that the anthropogenic pressure is on the mangrove, which plays a role of buffer between the village and the beach. The results from this vulnerability index highlight the need to protect coastal ecosystems in less vulnerable locations (such as Bandrélé) in order to maintain their protective role for the shore, and to restore or change the way to manage vulnerable coastal sites (such as M'tsamboro) in order to give them a better protection against natural and anthropogenic hazards.

To develop this vulnerability index, we were initially inspired by the coastal vulnerability index (CVI) presented by Hereher (2016). As it was not possible to replicate exactly the method from this study (due to practical constraints and local conditions), we developed a similar index based on the data available for our study sites and on the data that we could gather on the field and calculate by ourselves. We then looked for other similar indexes in the literature in order to be as comprehensive as possible and completed our index with complementary criteria from other studies (Bodéré et al., 1991; Gornitz et al., 1994; Cazes-Duvat, 2001; García-Mora et al., 2001; Williams et al., 2001; Jeanson, 2004; Alexandrakis and Poulos, 2014; Peña-Alonso et al., 2017; Ruol et al., 2018; Mathew et al., 2020). The goal of using this method was to obtain an index that takes into account a maximum of factors influencing beach vulnerability, while being adaptable to any situation. The adaptability of this index is an advantage because it can be relevant to any specific situations, but the counterpart is that the index is not standardised at a worldwide scale. It would therefore be difficult to compare this index between several studies. Harmonisation would be necessary in the boundary and threshold values used to score the criteria to obtain an "absolute" vulnerability to be able to compare several studies using this index. Indeed, the vulnerability index in our study reflects the relative vulnerability of the four study sites, not an absolute vulnerability.

The vulnerability index developed in this study focuses on the vulnerability of the beaches themselves. This was the choice made in this study, notably based on criteria inspired from literature, available data and scope of this study, but it is not the only way to grasp this concept. To highlight the need to protect natural ecosystems, another way is to assess their own vulnerability to climatic and anthropogenic hazards (as in the study from Hereher, 2016). In the ecological index from this study, coastal ecosystems (coral reefs, mangroves, seagrass beds) are only seen as factors protecting the shoreline and therefore decreasing its vulnerability (Table 2). However, these ecosystems can be seen as vulnerable themselves, therefore increasing the site vulnerability. In this other point of view, complementary data would be necessary (e.g., mangrove and coral reef diversity, density, etc.). One can argue that the density or width of mangroves also influences their protective role of the shore. There is no impact of this missing data in this study because the mangrove was present in only one site, but it could indeed be useful for any other study comparing several sites with mangroves. Several studies were already conducted about the impact of morpho- and hydrodynamic factors on mangroves in Mayotte (e.g., Jeanson et al., 2014, 2019). The coastal protective role of mangroves by the dissipation of wave energy and sediment stabilisation has been demonstrated in other studies (e.g., Spalding et al., 2014; Guannel et al., 2016; Narayan et al., 2016; Powell et al., 2019), but none of them is conducted specifically on Mayotte's mangroves. Another choice that can be made is to focus the assessment on the vulnerability of human assets. In this case, it would be of interest to analyse more precisely the infrastructures with cultural and socio-economic data (their exposure, susceptibiliy, and adaptability) as values to protect, and not only as pressures on the environment. Regarding the weighting coefficient given to the criteria in the calculation of each sub-index, and to the sub-indexes in the calculation of the multidisciplinary index, the choice was made not to give weights to the majority of the criteria and sub-indices, as in the study from Cazes-Duvat (2001). The only weighting factors provided were to give less weight to intelinked ecological criteria. An improvement of this method might be to ask the judgement from a panel of experts to choose relevant weighting factors for criteria and sub-indexes, as suggested in the study from Bagdanavičiūtė et al. (2015) using the analytical hierarchical process (AHP).

This method seems to be more accurate when the necessary data and experts are available (Bagdanavičiūtė et al., 2015).

In the context of Mayotte, it is also of interest to extent the vulnerability analysis to the whole island and to map it to make it more visually impacting for authorities. It would then be useful as a decision tool to prioritise sites to act on in coastal management. The anthropogenic sub-index shows that urbanisation can impact negatively the vulnerability of the shoreline. The changes in shoreline category over time shows that Mayotte's shoreline is subject to artificialisation, but in a moderate way. To prevent future intensive artificialisation and its impact on the shoreline and coastal ecosystems, conservation measures must be implemented as of now. In another context, it would be also interesting to adapt the index at a larger scale, e.g., the region or the world (to compare several islands in different oceans for example). In this last case, it is interesting to add a climatic sub-index with forcing variables contributing to coastal impacts, in particular erosion (such as in the study from Gornitz et al., 1994). The vulnerability index used in this study is therefore adaptable and can be used in all contexts and scales by adapting the boundary values of each criterion inside the indexes. The advantage of a multidisciplinary index is that it is not limited to one kind of factors and can therefore reflect a more integrative approach taking into account the vulnerability linked to various fields of science. Some criteria in this study were assessed qualitatively because of the availability of data, but another study could use only quantitatively determined criteria if sufficient resources are available.

## 5. Conclusions

The historical analysis of a time series of aerial photographs of Mayotte from 1950 to 2016 showed that the urbanisation of the shoreline is still low nowadays compared with the worldwide trend. However, the coastal development sped up in the last 30 years. At the scale of this study, natural environments (rocky shore, beach, and mangrove) did not show global trend of erosion or accretion, but it was observed that beaches and mangroves are more dynamic than rocky shores. With the increasing demographic pressure and socio-economic development in Mayotte, coastal habitats sheltering a rich biodiversity (e.g., coral reefs, beaches, mangroves, and seagrass beds) will probably be subject to more anthropogenic pressure in the future. It would therefore be advisable to manage the development in a sustainable way in order to preserve terrestrial, coastal, and marine environments in and around the island, with initiatives similar to the creation of the Mayotte Marine Natural Park for example. The use of a multidisciplinary vulnerability index could be helpful in the decisional process in the context of coastal management to take into account factors from several fields that influence vulnerability of ecosystems (beaches in the case of this study). The vulnerability index developed and used in this study is simple to make, can be adapted according to the available data, can include factors from different fields, and produces a unique value that can be communicated to authorities and coastal managers to help assess priorities in actions to undertake (e.g., restore vulnerable sites, and preserve less vulnerable sites). In the case of Mayotte, the vulnerability index demontrates the importance to preserve natural protective ecosystems (i.e., mangroves, coral reefs, and seagrass beds) and to use a sustainable management in the development of urban coastal areas in order to avoid an increase in the vulnerability of coastal sites.

**Funding:**

This work was supported by Fondation de France (2019-08602), ANR-19-CE34-0006-Manini, ANR-19-CE14-0010-SENSO.

**Acknowledgments:**

We wish to acknowledge the Fondation de France for supporting the project “Quel littoral demain dans l'Outre-mer Français”. We also acknowledge Sarah Charroux and Yann Mercky for their help during data acquisition on the field and data treatment.

**Declaration of Interests:**

The authors declare that they have no known competing financial interests or personal relationships that could have appeared to influence the work reported in this paper.

## References

Adger, W.N., Hughes, T.P., Folke, C., Carpenter, S.R., Rockström, J., 2005. Social-Ecological Resilience to Coastal Disasters. Science 309, 1036–1039. https://doi.org/10.1126/science.1112122

Airoldi, L., Beck, M.W., 2007. Loss, status and trends for coastal marine habitats of Europe, in: Oceanography and Marine Biology: An Annual Review. CRC Press, pp. 345–405.

Alexandrakis, G., Poulos, S., 2014. An holistic approach to beach erosion vulnerability assessment. Scientific reports 4, 6078. https://doi.org/10.1038/srep06078

Bagdanavičiūtė, I., Kelpšaitė, L., Soomere, T., 2015. Multi-criteria evaluation approach to coastal vulnerability index development in micro-tidal low-lying areas. Ocean & Coastal Management 104, 124–135. https://doi.org/10.1016/j.ocecoaman.2014.12.011

Bernardie-Tahir, N., El-Mahaboubi, O., 2001. Mayotte : des parfums au tourisme. Les nouveaux enjeux du littoral. Les Cahiers d'Outre-Mer. Revue de géographie de Bordeaux 54, 369–396. https://doi.org/10.4000/com.1137

Besset, M., Gratiot, N., Anthony, E.J., Bouchette, F., Goichot, M., Marchesiello, P., 2019. Mangroves and shoreline erosion in the Mekong River delta, Viet Nam. Estuarine, Coastal and Shelf Science 226, 106263. https://doi.org/10.1016/j.ecss.2019.106263

Boak, E.H., Turner, I.L., 2005. Shoreline Definition and Detection: A Review. Journal of Coastal Research 214, 688–703. https://doi.org/10.2112/03-0071.1

Bodéré, J.-C., Cribb, R., Curr, R., Davies, P., Hallégouët, B., Meur-Férec, C., Piriou, N., Williams, A., Yoni, C., 1991. La gestion des milieux dunaires littoraux. Evolution de leur vulnérabilité à partir d'une liste de contrôle. Etude de cas dans le sud du Pays de Galles et en Bretagne occidentale. Norois 151, 279–298. https://doi.org/10.3406/noroi.1991.6371

Cazes-Duvat, V., 2001. Évaluation de la vulnérabilité des plages à l'érosion : application à l'archipel des Seychelles / A beach vulnerability index and its implementation in the islands of Seychelles. Géomorphologie : relief, processus, environnement 7, 31–40. https://doi.org/10.3406/morfo.2001.1084

Chevalier, C., Devenon, J.L., Pagano, M., Rougier, G., Blanchot, J., Arfi, R., 2017. The atypical hydrodynamics of the Mayotte Lagoon (Indian Ocean): Effects on water age and potential impact on plankton productivity. Estuarine, Coastal and Shelf Science 196, 182–197. https://doi.org/10.1016/j.ecss.2017.06.027

Cohn, N., Anderson, D., Ruggiero, P., 2015. Observations of intertidal bar welding along a high energy, dissipative coastline, in: Coastal Sediments 2015. World Scientific. https://doi.org/10.1142/9789814689977_0021

Collin, A., Duvat, V., Pillet, V., Salvat, B., James, D., 2018. Understanding Interactions between Shoreline Changes and Reef Outer Slope Morphometry on Takapoto Atoll (French Polynesia). Journal of Coastal Research 85, 496–500. https://doi.org/10.2112/SI85-100.1

Cooper, J.A.G., Jackson, D.W.T., 2019. Coasts in Peril? A Shoreline Health Perspective. Frontiers in Earth Science 7. https://doi.org/10.3389/feart.2019.00260

De La Torre, Y., Aubie, S., 2003. Etude de la morpho-dynamique des littoraux de Mayotte. Phase 1 : synthèse, typologie et tendances d'évolution. (Rapport BRGM/RP-52320-FR).

Dolan, R., Hayden, B.P., May, P., May, S.K., 1980. The reliability of shoreline change measurements from aerial photographs. Shore and Beach 48, 22–29.

Dugan, J.E., Airoldi, L., Chapman, M.G., Walker, S.J., Schlacher, T., 2011. Estuarine and Coastal Structures: Environmental Effects, A Focus on Shore and Nearshore Structures, in: Wolanski, E., McLusky,

D. (Eds.), Treatise on Estuarine and Coastal Science. Academic Press, Waltham, pp. 17–41. https://doi.org/10.1016/B978-0-12-374711-2.00802-0

Duvat, V.K.E., Pillet, V., 2017. Shoreline changes in reef islands of the Central Pacific: Takapoto Atoll, Northern Tuamotu, French Polynesia. Geomorphology 282, 96–118. https://doi.org/10.1016/j.geomorph.2017.01.002

Gairin, E., Collin, A., James, D., Maueau, T., Roncin, Y., Lefort, L., Dolique, F., Jeanson, M., Lecchini, D., 2021. Spatiotemporal Trends of Bora Bora's Shoreline Classification and Movement Using High-Resolution Imagery from 1955 to 2019. Remote Sensing 13, 4692. https://doi.org/10.3390/rs13224692

Gallop, S.L., Young, I.R., Ranasinghe, R., Durrant, T.H., Haigh, I.D., 2014. The large-scale influence of the Great Barrier Reef matrix on wave attenuation. Coral Reefs 33, 1167–1178. https://doi.org/10.1007/s00338-014-1205-7

García-Mora, M.R., Gallego-Fernández, J.B., Williams, A.T., García-Novo, F., 2001. A Coastal Dune Vulnerability Classification. A Case Study of the SW Iberian Peninsula. Journal of Coastal Research 17, 802–811.

Giraud-Renard, E., Dolique, F., Collin, A., James, D., Gairin, E., Courteille, M., Beaufort, O., René-Trouillefou, M., Dulormne, M., Jeanson, M., Lecchini, D., 2022. Long-term evolution of the Guadeloupean shoreline (1950-2017). Journal of Coastal Research. http://dx.doi.org/10.2112/JCOASTRES-D-21-00161.1.

Gittman, R.K., Scyphers, S.B., Smith, C.S., Neylan, I.P., Grabowski, J.H., 2016. Ecological Consequences of Shoreline Hardening: A Meta-Analysis. BioScience 66, 763–773. https://doi.org/10.1093/biosci/biw091

Gornitz, V.M., Daniels, R.C., White, T.W., Birdwell, K.R., 1994. The Development of a Coastal Risk Assessment Database: Vulnerability to Sea-Level Rise in the U.S. Southeast. Journal of Coastal Research Special issue, 327–338.

Guannel, G., Arkema, K., Ruggiero, P., Verutes, G., 2016. The Power of Three: Coral Reefs, Seagrasses and Mangroves Protect Coastal Regions and Increase Their Resilience. PLOS ONE 11, e0158094. https://doi.org/10.1371/journal.pone.0158094

Hapke, C.J., Himmelstoss, E.A., Kratzmann, M.G., List, J.H., Thieler, E.R., 2011. National Assessment of Shoreline Change: Historical Shoreline Change along the New England and Mid-Atlantic Coasts (Open-File Report 2010-1118), Open-File Report. U.S. Geological Survey.

Hereher, M.E., 2016. Vulnerability assessment of the Saudi Arabian Red Sea coast to climate change. Environ Earth Sci 75, 13. https://doi.org/10.1007/s12665-015-4835-3

Idier, D., Romieu, E., Delattre, M., Pedreros, R., de la Torre, Y., 2008. Hydrodynamique tidale du lagon de Mayotte : observations in situ et modélisation, in: Xèmes Journées, Sophia Antipolis. Presented at the Journées Nationales Génie Côtier - Génie Civil, Editions Paralia, pp. 553–562. https://doi.org/10.5150/jngcgc.2008.053-I

INSEE, 2017. Recensement de la population à Mayotte [WWW Document]. URL https://www.insee.fr/fr/statistiques/3291775?sommaire=2120838

IPCC, 2019. IPCC Special Report on the Ocean and Cryosphere in a Changing Climate.

Jeanson, M., 2004. Dynamique morphosédimentaire en milieu récifal et lagonaire, Etude de cas aux îles de Tahiti et Moorea (Polynésie française). Université de Reims Champagne-Ardenne.

Jeanson, M., 2009. Morphodynamique du littoral de Mayotte, des processus au réseau de surveillance. Université du Littoral Côte d'Opale.

Jeanson, M., Anthony, E.J., Dolique, F., Aubry, A., 2013. Wave characteristics and morphological variations of pocket beaches in a coral reef–lagoon setting, Mayotte Island, Indian Ocean. Geomorphology 182, 190–209. https://doi.org/10.1016/j.geomorph.2012.11.013

Jeanson, M., Anthony, E.J., Dolique, F., Cremades, C., 2014. Mangrove Evolution in Mayotte Island, Indian Ocean: A 60-year Synopsis Based on Aerial Photographs. Wetlands 34, 459–468. https://doi.org/10.1007/s13157-014-0512-7

Jeanson, M., Dolique, F., Anthony, E.J., Aubry, A., 2019. Decadal-scale Dynamics and Morphological Evolution of Mangroves and Beaches in a Reef-lagoon Complex, Mayotte Island. Journal of Coastal Research 88, 195. https://doi.org/10.2112/SI88-015.1

Kench, P.S., Brander, R.W., 2006. Wave Processes on Coral Reef Flats: Implications for Reef Geomorphology Using Australian Case Studies. Journal of Coastal Research 22, 209–223. https://doi.org/10.2112/05A-0016.1

Kindermann, G., Gormally, M.J., 2010. Vehicle damage caused by recreational use of coastal dune systems in a Special Area of Conservation (SAC) on the west coast of Ireland. Journal of Coastal Conservation 14, 173–188. https://doi.org/10.1007/s11852-010-0102-7

Le Berre, I., 2017. L'artificialisation des littoraux : déterminants et impacts, in: Béchet, B., Le Bissonais, Y., Ruas, A. (Eds.), Sols Artificialisés et Processus d'artificialisation Des Sols : Déterminants, Impacts et Leviers d'action. Expertise Scientifique Collective (ESCo). IFSTTAR, INRA, pp. 234–254.

Lee, J.-T., Yen, L.-Z., Chu, M.-Y., Lin, Y.-S., Chang, C.-C., Lin, R.-S., Chao, K.-H., Lee, M.-J., 2020. Growth Characteristics and Anti-Wind Erosion Ability of Three Tropical Foredune Pioneer Species for Sand Dune Stabilization. Sustainability 12, 3353. https://doi.org/10.3390/su12083353

Leone, F. (dir) et al., 2014. Atlas des risques naturels et des vulnérabilités territoriales de Mayotte, collection “Géorisques”, hors-série. PULM, Montpellier.

Letortu, P., Costa, S., Maquaire, O., Delacourt, C., Augereau, E., Davidson, R., Suanez, S., 2014. Taux d’ablation des falaises crayeuses haut-normandes : l’apport du scanner laser terrestre, in: Géomorphologie : relief, processus, environnement. Presented at the Actes des 14e Journées des Jeunes Géomorphologues, Groupe français de géomorphologie (GFM), pp. 133–144. https://doi.org/10.4000/geomorphologie.10872

Liu, B., Gong, M., Wu, X., Liu, X., 2021. A comprehensive model of vessel anchoring pressure based on machine learning to support the sustainable management of the marine environments of coastal cities. Sustainable Cities and Society 72, 103011. https://doi.org/10.1016/j.scs.2021.103011

Madi Moussa, R., Fogg, L., Bertucci, F., Calandra, M., Collin, A., Aubanel, A., Polti, S., Benet, A., Salvat, B., Galzin, R., Planes, S., Lecchini, D., 2019. Long-term coastline monitoring on a coral reef island (Moorea, French Polynesia). Ocean & Coastal Management 180, 104928. https://doi.org/10.1016/j.ocecoaman.2019.104928

Masse, J.P., Thomassin, B.A., Acquaviva, M., 1989. Bioclastic Sedimentary Environments of Coral Reefs and Lagoon around Mayotte Island (Comoro Archipelago, Mozambique Channel, SW Indian Ocean). Journal of Coastal Research 5, 419–432.

Mathew, M.J., Sautter, B., Ariffin, E.H., Menier, D., Ramkumar, M., Siddiqui, N.A., Delanoe, H., Del Estal, N., Traoré, K., Gensac, E., 2020. Total vulnerability of the littoral zone to climate change-driven natural hazards in north Brittany, France. Science of The Total Environment 706, 135963. https://doi.org/10.1016/j.scitotenv.2019.135963

Matić-Skoko, S., Vrdoljak, D., Uvanović, H., Pavičić, M., Tutman, P., Bojanić Varezić, D., 2020. Early evidence of a shift in juvenile fish communities in response to conditions in nursery areas. Sci Rep 10, 21078. https://doi.org/10.1038/s41598-020-78181-w

Météo-France, 2021. Climat Mayotte. URL http://www.meteofrance.yt/climat/mayotte

Narayan, S., Beck, M.W., Reguero, B.G., Losada, I.J., Wesenbeeck, B. van, Pontee, N., Sanchirico, J.N., Ingram, J.C., Lange, G.-M., Burks-Copes, K.A., 2016. The Effectiveness, Costs and Coastal Protection Benefits of Natural and Nature-Based Defences. PLOS ONE 11, e0154735. https://doi.org/10.1371/journal.pone.0154735

Nordstrom, K.F., 2004. Beaches and Dunes of Developed Coasts. Cambridge University Press.

Nougier, J., Cantagrel, J.M., Karche, J.P., 1986. The Comores archipelago in the western Indian Ocean: volcanology, geochronology and geodynamic setting. Journal of African Earth Sciences (1983) 5, 135–145. https://doi.org/10.1016/0899-5362(86)90003-5

Ondiviela, B., Losada, I.J., Lara, J.L., Maza, M., Galván, C., Bouma, T.J., van Belzen, J., 2014. The role of seagrasses in coastal protection in a changing climate. Coastal Engineering 87, 158–168. https://doi.org/10.1016/j.coastaleng.2013.11.005

Oyedotun, T.D.T., 2014. Shoreline geometry: DSAS as a tool for Historical Trend Analysis. Geomorphological Techniques (Online Edition) 2, 1–12.

Peña-Alonso, C., Fraile-Jurado, P., Hernández-Calvento, L., Pérez-Chacón, E., Ariza, E., 2017. Measuring geomorphological vulnerability on beaches using a set of indicators (GVI): A tool for management. Journal of Environmental Management 204, 230–245. https://doi.org/10.1016/j.jenvman.2017.08.053

Powell, E.J., Tyrrell, M.C., Milliken, A., Tirpak, J.M., Staudinger, M.D., 2019. A review of coastal management approaches to support the integration of ecological and human community planning for climate change. J Coast Conserv 23, 1–18. https://doi.org/10.1007/s11852-018-0632-y

Rault, C., Dewez, T.J.B., Aunay, B., 2020. Structure-from-motion processing of aerial photographs: sensitivity analyses pave the way for quantifying geomorphological changes since 1978 in La Réunion

Island. ISPRS Ann. Photogramm. Remote Sens. Spatial Inf. Sci. V-2–2020, 773–780. https://doi.org/10.5194/isprs-annals-V-2-2020-773-2020

Ray, G.C., Hayden, B.P., 1992. Coastal Zone Ecotones, in: Hansen, A.J., di Castri, F. (Eds.), Landscape Boundaries: Consequences for Biotic Diversity and Ecological Flows, Ecological Studies. Springer, New York, NY, pp. 403–420. https://doi.org/10.1007/978-1-4612-2804-2_21

Robbe, E., Woelfel, J., Balčiūnas, A., Schernewski, G., 2021. An Impact Assessment of Beach Wrack and Litter on Beach Ecosystem Services to Support Coastal Management at the Baltic Sea. Environmental Management 68, 835–859. https://doi.org/10.1007/s00267-021-01533-3

Ruol, P., Martinelli, L., Favaretto, C., 2018. Vulnerability Analysis of the Venetian Littoral and Adopted Mitigation Strategy. Water 10, 984. https://doi.org/10.3390/w10080984

Simeone, S., Palombo, A.G.L., Guala, I., 2012. Impact of frequentation on a Mediterranean embayed beach: Implication on carrying capacity. Ocean & Coastal Management 62, 9–14. https://doi.org/10.1016/j.ocecoaman.2012.02.011

Spalding, M.D., Ruffo, S., Lacambra, C., Meliane, I., Hale, L.Z., Shepard, C.C., Beck, M.W., 2014. The role of ecosystems in coastal protection: Adapting to climate change and coastal hazards. Ocean & Coastal Management 90, 50–57. https://doi.org/10.1016/j.ocecoaman.2013.09.007

Tuholske, C., Halpern, B.S., Blasco, G., Villasenor, J.C., Frazier, M., Caylor, K., 2021. Mapping global inputs and impacts from of human sewage in coastal ecosystems. PLOS ONE 16, e0258898. https://doi.org/10.1371/journal.pone.0258898

Turner, R.K., Schaafsma, M. (eds.), 2015. Coastal Zones Ecosystem Services: From Science to Values and Decision Making, Springer. ed, Studies in Ecological Economics. Switzerland.

United Nations, 2017. Factsheet: People and Oceans, in: Ocean Fact Sheet Package. Presented at the Ocean Conference, New York, pp. 1–7.

Williams, A.T., Alveirinho-Dias, J., Garcia Novo, F., García-Mora, M.R., Curr, R., Pereira, A., 2001. Integrated coastal dune management: checklists. Continental Shelf Research, European Land-Ocean Interaction 21, 1937–1960. https://doi.org/10.1016/S0278-4343(01)00036-X